0888-8809/07/$15.00/0
Printed in U.S.A.

Molecular Endocrinology 21(10):2472–2486

doi: 10.1210/me.2007-0147

SMAD3 Regulates Gonadal Tumorigenesis

Qinglei Li, Jonathan M. Graff, Anne E. O'Connor, Kate L. Loveland, and Martin M. Matzuk

Departments of Pathology (Q.L., M.M.M.), Molecular and Human Genetics (M.M.M.), Molecular and Cellular Biology (M.M.M.), Baylor College of Medicine, Houston, Texas 77030; Department of Developmental Biology (J.M.G.), University of Texas Southwestern Medical Center, Dallas, Texas 75390; and Monash Institute of Medical Research (A.E.O., K.L.L.), Monash University, Clayton, Victoria 3168, Australia

Inhibin is a secreted tumor suppressor and an activin antagonist. Inhibin α null mice develop gonadal sex cord-stromal tumors with 100% penetrance and die of a cachexia-like syndrome due to increased activin signaling. Because Sma and Mad-related protein (SMAD)2 and SMAD3 transduce activin signals *in vitro*, we attempted to define the role of SMAD3 in gonadal tumorigenesis and the wasting syndrome by generating inhibin α and *Smad3* double mutant mice. Inhibin α and *Smad3* double homozygous males were protected from early tumorigenesis and the usual weight loss and death. Approximately 90% of these males survived to 26 wk in contrast to 95% of inhibin-deficient males, which develop bilateral testicular tumors and die of the wasting syndrome by 12 wk. Testicular tumors were either absent or unilaterally slow growing and less hemorrhagic in the majority of double-knockout males. In contrast, development of the ovarian tumors and wasting syndrome was delayed, but still occurred, in the majority of the double-knockout females by 26 wk. In double mutant females, tumor development was accompanied by typical activin-induced pathological changes. In summary, we identify an important function of SMAD3 in gonadal tumorigenesis in both sexes. However, this effect is significantly more pronounced in the male, indicating that SMAD3 is the primary transducer of male gonadal tumorigenesis, whereas SMAD3 potentially overlaps with SMAD2 function in the ovary. Moreover, the activin-induced cachexia syndrome is potentially mediated through both SMAD2 and SMAD3 or only through SMAD2 in the liver and stomach. These studies identify sexually dimorphic functions of SMAD3 in gonadal tumorigenesis. (*Molecular Endocrinology* 21: 2472–2486, 2007)

ACTIVINS AND INHIBINS are secreted TGF-β superfamily ligands that orchestrate a host of normal physiological and developmental processes (1–3). Activins are disulfide-linked homodimers or heterodimers of β-subunits and include activin A (βA: βA), activin B (βB: βB), and activin AB (βA: βB) (4), whereas inhibins are disulfide-linked heterodimers of α and β subunits [inhibin A (α: βA) and inhibin B (α: βB)] that antagonize activin signaling by acting as activin receptor (ActR) antagonists (5). Both activins and inhibins are expressed in multiple tissues including pituitary gonadotropes, Sertoli cells of the testis, and ovarian granulosa cells (6–8). Although activins and inhibins were initially found as regulators of pituitary FSH biosynthesis and secretion (6, 9), subsequent studies identified diverse functions including regulation of proliferation, differentiation, and development (10–13).

Genetic approaches have helped to more fully define the functional role of inhibins (14). Male and female mice homozygous for an inhibin α (*Inha*) null allele (*i.e*. deficient in inhibins) develop multifocal and hemorrhagic gonadal sex cord-stromal tumors as early as 4 wk of age with essentially 100% penetrance, thus identifying inhibin as a secreted tumor suppressor (14). Inhibin is also an adrenal tumor suppressor because castrated (gonadectomized) inhibin-deficient mice invariably develop adrenal tumors after 20 wk of age (15). The inhibin-deficient mice succumb to a cachexia-like wasting syndrome (*i.e*. weight loss, lethargy, hunchback, sunken-eye appearance, pale periphery, kyphoscoliosis, *etc*.) and have elevated serum activin and estradiol (E_2) levels (15, 16). The cachexia is secondary to activin signaling because it is minimized in *Inha* and *ActRII* double mutant mice (17).

Activins signal through ActRs (ActRIIA and ActRIIB) and ActR-like kinases (type I receptors), leading to the phosphorylation and activation of the receptor-regulated SMADs (R-SMADs; SMAD2 and SMAD3) (2, 18–23). Heteromeric complexes are then formed between the activated SMAD2-SMAD3 and common SMAD (SMAD4). The complexes subsequently translocate to the nucleus to regulate gene expression in a cell-specific pattern via recruitment of distinct transcription factors, coactivators, and corepressors (1, 3, 24–27). Although SMAD2 and SMAD3 share more than 90% identity in their amino acids, functional and structural differences have been demonstrated between SMAD2

First Published Online June 26, 2007

Abbreviations: ActR, Activin receptor; E_2, estradiol; WT, wild type.

***Molecular Endocrinology* is published monthly by The Endocrine Society (http://www.endo-society.org), the foremost professional society serving the endocrine community.**

and SMAD3. *In vitro* studies have suggested that SMAD3, but not SMAD2, plays a role in the transcriptional activation of the rat *FSHβ* promoter (28) although there is some debate about the role of SMAD2 in this process (29). Mice with *Smad2* loss of function are embryonic lethal (30–34) whereas *Smad3* knockout mice are viable but develop colorectal cancer (35) and have immune defects (36).

The genesis of the gonadal tumorigenesis in inhibin-deficient mice is unknown. It is possible that it is the effect of, but not limited to, increased FSH, enhanced estrogen signaling, or potentiated activin signaling in the absence of inhibin. FSH is heterodimeric glycoprotein that is critically involved in the menstrual cycle and regulated in a series of complex feedback loops. Consistent with the role of inhibin in suppressing FSH production and secretion, *Inha* null mice have significantly elevated serum FSH levels (14). A role of FSH in regulating gonadal tumorigenesis was identified in our genetic mouse model, which lacks both FSH and inhibin (37). Similarly, E_2 levels are also increased in *Inha* null mice, and estrogen signaling plays a critical role in promoting tumor progression in inhibin-deficient male mice (38). Support for the involvement of activin signaling in gonadal tumorigenesis stems from *in vitro* evidence that growth of gonadal tumor cells was stimulated by activins (39). However, direct *in vivo* evidence establishing this link is lacking, because mice lacking both activin βA and βB (deficient in both activins and inhibins) die within 24 h of birth secondary to multiple abnormalities in craniofacial development (23), precluding the possibility to directly examine the roles of activins in gonadal tumor development in inhibin-deficient mice. However, SMAD2 and SMAD3 transduce activin signals, and gonadal tumors in inhibin-deficient mice are derived from the granulosa/Sertoli cell lineages (14), cells that express both activin-responsive SMADs, SMAD2 and SMAD3 (40–44), the roles of which in gonadal tumorigenesis as well as activin-induced cachexia remain unknown. Because *Smad3* mutant mice are viable, it was possible to examine the roles of activin-responsive SMAD3 in the development of gonadal tumors. For these reasons, we generated *Inha* and *Smad3* double mutant mice to help delineate the roles of activin-responsive SMADs in gonadal tumorigenesis and the development of the wasting syndrome.

We found in the current studies that *Inha* and *Smad3* double homozygous mutant males were protected from early tumorigenesis, weight loss, and death. The majority of double mutants survived beyond 26 wk, and the testicular tumors were either absent or unilateral, slow growing, and less hemorrhagic. SMAD3 deficiency also reduced female ovarian tumorigenesis but to a much milder degree than in males. These results provide fundamental *in vivo* evidence to help in understanding the contributions of SMAD-related signaling in gonadal tumorigenesis.

RESULTS

SMAD3 Is an Important Genetic Modifier in Testicular Tumorigenesis

To begin to study the role of SMAD3 in inhibin-deficient mice, we generated and then intercrossed *Smad3;Inha* double heterozygotes. We separated the sexes into two cohorts and first examined the males. As a first step, we evaluated survival curves as a potential indicator of tumorigenesis. We found that loss of SMAD3 substantially prolonged the lifespan of inhibin-deficient mice and potentially in a dosage-sensitive fashion (Fig. 1A). The survival curve (Fig. 1A) showed 50% of *Inha*$^{-/-}$*;Smad3* wild-type (WT) male mice died by 10.5 wk of age. Heterozygosity at the *Smad3* locus extended the 50% survival to approximately 14.5 wk, but by 17 wk the curves were overlapping. Remarkably, all of the double homozygous males survived beyond 12 wk of age, and 90% of them survived to 26 wk, mirroring control *Smad3*$^{-/-}$*;Inha* WT mice. At this time point, the studies were terminated so that the gonads of the double homozygotes could be examined. One *Inha*$^{-/-}$*;Smad3*$^{-/-}$ male and one *Smad3*$^{-/-}$ male were killed at 21 and 25 wk of age, respectively, due to the presence of rectal prolapse and the development of colorectal cancer, a phenotype secondary to SMAD3 deficiency (35).

Because the survival curves indicated a possible attenuation of the inhibin-deficient tumor phenotype, the double homozygotes (n = 9) were examined at 26 wk of age. Strikingly, around 40% of the mice did not develop macro- and microscopic testicular tumors. Some of these animals did have enlarged testes with (data not shown) or without the presence of cyst(s) (Fig. 1, B and E). The majority of the remaining 60% developed unilaterally small tumors that were less hemorrhagic with a few tumor foci that could be detected with serial sections (Fig. 1, B, F, and G). Occasionally, the contralateral testis developed cyst(s). Figure 1H depicts the testicular tumor in a 21-wk-old double-knockout male that was killed due to the presence of a colorectal cancer. The only other exception in these double-knockout mice was that one 26-wk-old double homozygous male developed a relatively hemorrhagic tumor in one testis. The above findings are in sharp contrast with the *Inha*$^{-/-}$ males, which inevitably developed bilateral hemorrhagic and aggressive tumors that encompassed the entirety of both testes (Fig. 1, B and C). All of the *Inha*$^{-/-}$*;Smad3*$^{+/-}$ and *Inha*$^{-/-}$ males in this experiment developed sex cord-stromal tumors by 26 wk. However, about 20% of the *Inha*$^{-/-}$*;Smad3*$^{+/-}$ males developed unilateral tumors. Analysis of the testis weights showed that the average weight of testes from both 10- and 26-wk-old double-knockout males was lower than that from the *Inha*$^{-/-}$ males at the advanced stage of tumor progression (Fig. 1I, $P < 0.05$). To delineate a time line of tumorigenesis in the double-knockout males, we analyzed their testes at 6 (n = 3), 10 (n = 5), 12 (n = 1),

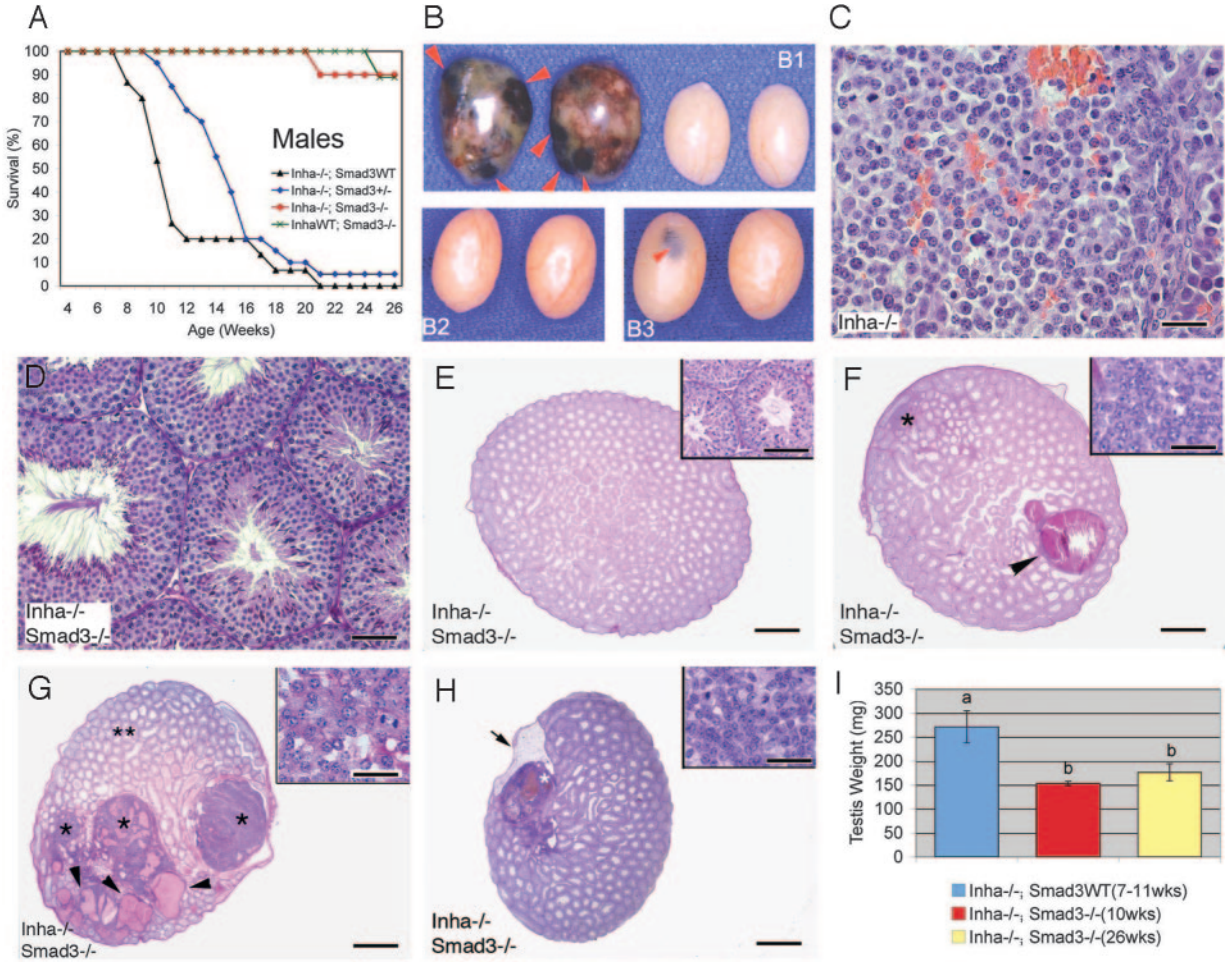

Fig. 1. SMAD3 Is an Important Genetic Modifier in Testicular Tumor Development

A, Survival curve of *Inha*$^{-/-}$ (n = 15), *Inha*$^{-/-}$;*Smad3*$^{+/-}$ (n = 20), *Inha*$^{-/-}$;*Smad3*$^{-/-}$ (n = 10), and *Inha* WT;*Smad3*$^{-/-}$ (n = 9) male mice. B, Testes from a 10-wk-old *Inha*$^{-/-}$ male (B1, *left*) were hemorrhagic (*arrowheads*) and significantly enlarged compared with testes from a 12-wk-old *Inha*$^{-/-}$;*Smad3*$^{-/-}$ male (B1, *right*), which had no tumor foci and were grossly normal. Panel B2 shows testes from an *Inha*$^{-/-}$;*Smad3*$^{-/-}$ male at 26 wk of age were free of tumor, whereas testes from another double-knockout male (B3) at the same age had a hemorrhagic focus (*arrowhead*) and a small tumor (histology in panel F). C, Representative histology of sex cord-stromal tumors developed in the *Inha*$^{-/-}$ male (B1, *left*). Note the presence of mitotically active tumor cells under high magnification. D, Representative histology of testes from a 12-wk-old double-knockout male (B1, *right*) with normal seminiferous tubule structure and the presence of spermatogenesis. E, Representative histology of testes from a 26-wk-old double-knockout male (B2) with normal testicular structure and the presence of spermatogenesis (*inset*). F, Histology of a testis (*left* testis in B3) from a 26-wk-old double-knockout male. Note the hemorrhage (*arrowhead*) and a small tumor (*) viewed under high magnification (*inset*). G, Representative histology of the testicular tumors developed in a 26-wk-old double-knockout male. Note the presence of more than one small tumors (*) and cysts (*arrowheads*) as well as abundant tubule structures (**) in the testis. Spermatogenesis can still be found in some tubules of this testis (data not shown). The *inset* denotes the high-power view of one of the tumor foci (*), all of which contain mitotically active cells. H, Representative histology of the testes from a 21-wk-old double-knockout male that was killed because of the development of colorectal cancer. Note the presence of a small tumor (*) and a cyst (*arrow*) in the testis. The *inset* is a high-power view of the tumor (*). I, Average weight of testis from *Inha*$^{-/-}$ (7–11 wk; n = 10) and *Inha*$^{-/-}$;*Smad3*$^{-/-}$ males (n = 6 for both 10- and 26-wk groups). Note the average testis weight from *Inha*$^{-/-}$ males was higher than that from the double-knockout mice (10 wk and 26 wk) ($P < 0.05$). Data are shown as mean ± SEM, and *bars without a common superscript* are significantly different. *Scale bars*, C and *insets* in F–H, 25 μm; D, 50 μm; *inset* in E, 100 μm; E–H, 800 μm.

and 15 (n = 1) wk of age. No gross tumors were visible at any of these stages, and the testes were histologically indistinguishable from those of the WT mice with normal spermatogenesis (Fig. 1, B and D). In contrast, testes from *Inha*$^{-/-}$ males developed hemorrhagic tumors (Fig. 1, B and C).

Inha knockout males develop infertility secondary to testicular tumor development (16). To examine the reproductive potential of mice with both *Smad3* and *Inha* loss of function, *Inha*$^{-/-}$;*Smad3*$^{-/-}$ males (n = 2) at the age of 8 wk were mated with WT females. Both males sired offspring whose genotype was *Inha*$^{+/-}$;

Smad3$^{+/-}$, confirming the double homozygous genotype of the parent males. The fertility of *Inha*$^{-/-}$; *Smad3*$^{-/-}$ males was further evaluated by crossing the double-knockout males (n = 5) with the *Inha*$^{+/-}$; *Smad3*$^{+/-}$ females (n = 10; two females per breeding cage), and the double heterozygous males: n = 5) were used as controls (Table 1). All of the *Inha*$^{-/-}$; *Smad3*$^{-/-}$ males sired offspring, although they demonstrated reduced fertility during a 3-month test period with reduced number of litters (25 for double heterozygous and 14 for double knockout) and total progeny (175 for double heterozygous and 82 for double knockout). The average litter per female each month was markedly decreased for the *Inha*$^{-/-}$; *Smad3*$^{-/-}$ males compared with controls (0.47 ± 0.06 *vs.* 0.83 ± 0.05; $P < 0.01$), although the litter size was not significantly different compared with the DHET males (5.62 ± 1.05 *vs.* 5.96 ± 0.52; $P > 0.05$). Thus, loss of *Smad3* in the inhibin-deficient males partially rescued the fertility defects.

Absence of SMAD3 in the Inhibin-Deficient Background Forestalls the Usual Weight Loss and Associated Cachexia-Like Symptoms in Males

To determine the effect of absence of Smad3 on the cachexia-like syndrome, the weights of male mice with different genotypes (*Inha*$^{-/-}$*;Smad3* WT, *Inha*$^{-/-}$*;Smad3*$^{+/-}$, *Inha*$^{-/-}$*;Smad3*$^{-/-}$, and *Inha* WT; *Smad3*$^{-/-}$) were measured weekly for a period of 4–26 wk (Fig. 2A). Weight loss in inhibin-deficient male mice, an early sign of tumorigenesis, occurred approximately after 6–7 wk of age accompanied by dorsal kyphoscoliosis and a sunken-eye appearance. However, the weight loss and associated cachexia symptoms were minimal in *Inha*$^{-/-}$*;Smad3*$^{-/-}$ males during the 26-wk experimental period. Loss of one copy of Smad3 in the inhibin-deficient background also delayed the onset of weight loss as evidenced in *Inha*$^{-/-}$ *Smad3*$^{+/-}$ males, although these mice eventually became cachectic and demonstrated weight loss. Compared with *Smad3*$^{-/-}$ mice, the body weights of the double-knockout males seemed to plateau around 16 wk, which might reflect the effect of the presence of slow-growing tumors in some double-knockout males.

Because the cachexia-like syndrome was accompanied by pathological changes in the liver and stomach, these organs were examined histologically. Depletion of gastric parietal cells and hepatocellular necrosis around the central vein are two prominent histological hallmarks of cachectic inhibin-deficient mice (15). These pathological changes in the stomach were apparent in *Inha*$^{-/-}$; *Smad3* WT (Fig. 2B) and *Inha*$^{-/-}$;*Smad3*$^{+/-}$ (data not shown) males at the terminal stages. However, in the 10-, 12-, 14-, and 26-wk-old double homozygous males, parietal cells were present at normal levels, and no glandular atrophy was found (Fig. 2C). The pathological changes in the livers were found in the cachectic *Inha*$^{-/-}$;*Smad3* WT (Fig. 2D) and *Inha*$^{-/-}$;*Smad3*$^{+/-}$ (data not shown) males, but not in the 10-, 12-, 14-, and 26-wk-old double homozygous mutants (Fig. 2E). Consistent with the histological observations, liver weights were higher in *Inha*$^{-/-}$;*Smad3*$^{-/-}$ males at both 10 and 26 wk of age compared with *Inha*$^{-/-}$ males at the ages of 7–11 wk (Fig. 2F; $P < 0.01$). Anemia, another feature of inhibin deficiency-induced cachexia, was also not apparent in the double homozygous males at 10 and 26 wk of age (Fig. 2G).

Serum Activin A Levels Are Reduced in *Inha*$^{-/-}$*; Smad3*$^{-/-}$ Males

Tumors in inhibin-deficient mice produce substantial amount of activins, which significantly contribute to the highly elevated serum activin levels and lead to the severe cachexia-like syndrome (15, 17). Because the double-knockout males had markedly reduced tumor progression and demonstrated minimal cachexia, low serum activin levels are expected in these mice. Consistent with our previous findings (15), dramatically elevated activin A levels were found in the *Inha*$^{-/-}$ males compared with WT controls (Fig. 3A; $P < 0.01$). As expected, the *Inha*$^{-/-}$*;Smad3*$^{-/-}$ males at both 10 and 26 wk of age had significantly lower activin A levels (10 wk: 0.08 ± 0.01 ng/ml; 26 wk: 5.45 ± 3.58 ng/ml) compared with the Inha$^{-/-}$ males (30.08 ± 4.66 ng/ml; $P < 0.01$), which correlated with the tumor status in these double knockouts. Although the 26-wk-old *Inha*$^{-/-}$*;Smad3*$^{-/-}$ males have higher activin A levels than the 10-wk-old double knockouts, significance was not achieved ($P > 0.05$). Of note, activin A levels were not altered in *Smad3*$^{-/-}$ males (0.06 ± 0.01 ng/ml) compared with adult WT controls (0.05 ± 0.01 ng/ml; $P > 0.05$). These findings provide strong evidence that attenuation of the tumor phenotype in the double-knockout males contributes to the mechanism that leads to the reduced serum activin levels in this model.

Table 1. Three-Month Fertility Test Data for the *Inha*;*Smad3* Double-Mutant Mice

Genotype	No. of Males	Total Pups	Total Litters	Average Litter/Female/Month	Average Pups/Female/Litter
Inha$^{+/-}$;*Smad3*$^{+/-}$	5	175	25	0.83 ± 0.05[a]	5.96 ± 0.52
Inha$^{-/-}$;*Smad3*$^{-/-}$	5	82	14	0.47 ± 0.06[b]	5.62 ± 1.05

Each male mouse was caged with two *Inha*$^{+/-}$; *Smad3*$^{+/-}$ female mice. Data are shown as mean ± SEM.
[a] *vs.* [b], $P < 0.01$.

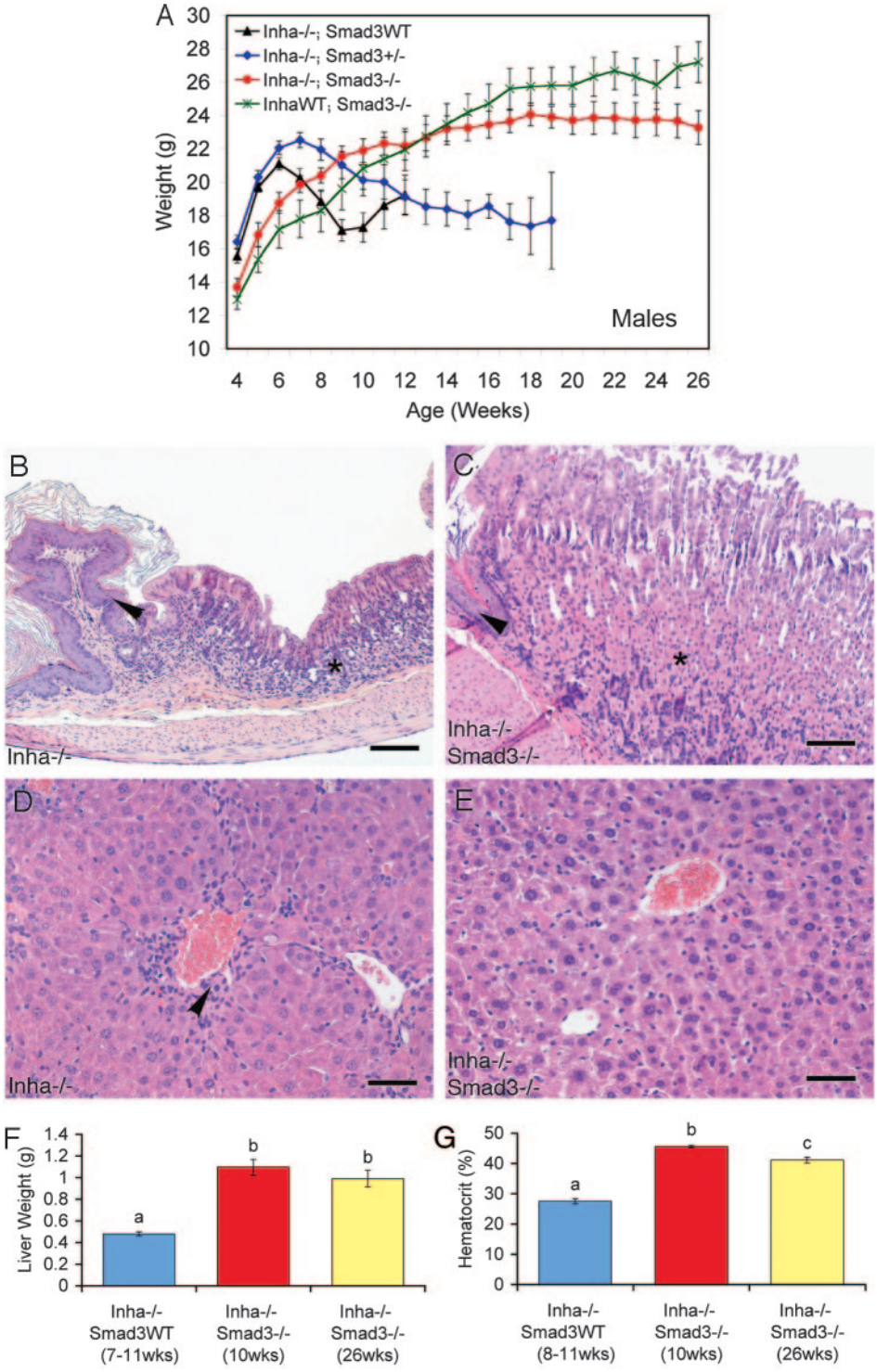

Fig. 2. Cachexia Wasting Syndrome Is Minimal in *Inha*$^{-/-}$;*Smad3*$^{-/-}$ Male Mice

A, The weight curves of *Inha*$^{-/-}$ (n = 15), *Inha*$^{-/-}$; *Smad3*$^{+/-}$ (n = 20), *Inha*$^{-/-}$;*Smad3*$^{-/-}$ (n = 10), and *Inha* WT;*Smad3*$^{-/-}$ (n = 9) males. Note the double-knockout males were protected from the severe weight loss that occurred in *Inha*$^{-/-}$ mice. B and C, Glandular stomachs from a 11-wk-old *Inha*$^{-/-}$ male with advanced testicular tumors and a 26-wk-old *Inha*$^{-/-}$; *Smad3*$^{-/-}$ male, respectively. Note that large, eosinophilic parietal cells are present in the glandular region of the stomach in the double-knockout male (C), whereas glandular atrophy and depletion of parietal cells were evident in *Inha*$^{-/-}$ mice (B). For orientation and comparison, the areas photographed in panels B and C depict the junction between the squamous epithelium of the forestomach (*arrowhead*) and the glandular region (*). D and E, Histological analyses of livers from a 7-wk-old *Inha*$^{-/-}$ male with advanced testicular tumors (D) and a 26-wk-old *Inha*$^{-/-}$;*Smad3*$^{-/-}$ male (E). Hepatocellular death around the central vein with scattered sites of necrosis and lymphocytic infiltration (*arrowhead*) are noted in the livers of *Inha*$^{-/-}$ male but not the double-knockout male.

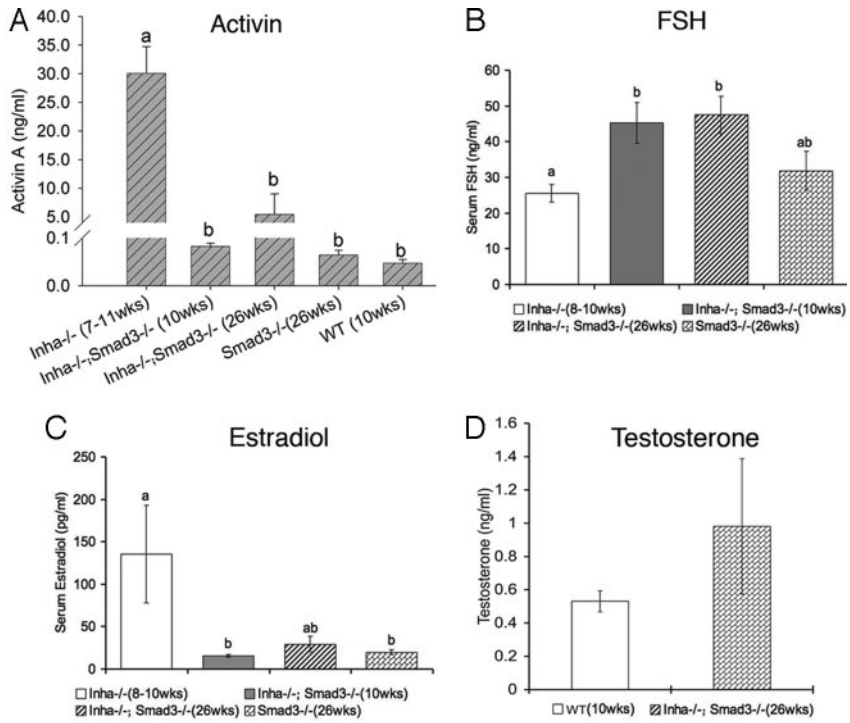

Fig. 3. Serum Activin A and Hormone Levels in the *Inha*$^{-/-}$;*Smad3*$^{-/-}$ Male Mice

A, Comparison of serum activin A levels among *Inha*$^{-/-}$, *Inha*$^{-/-}$;*Smad3*$^{-/-}$ (10 wk and 26 wk), *Smad3*$^{-/-}$, and WT males. Note the significantly lower activin A levels in *Inha*$^{-/-}$;*Smad3*$^{-/-}$ (10 wk and 26 wk) males compared with the *Inha*$^{-/-}$ males. B, Comparison of serum FSH levels among *Inha*$^{-/-}$, *Inha*$^{-/-}$; *Smad3*$^{-/-}$ (10 wk and 26 wk), and *Smad3*$^{-/-}$ mice. The higher FSH levels were found in the double-knockout males (10 and 26 wk) compared with *Inha*$^{-/-}$ males. C, Comparison of serum E_2 levels among *Inha*$^{-/-}$, *Inha*$^{-/-}$;*Smad3*$^{-/-}$, and *Smad3*$^{-/-}$ mice. Note the lower serum E_2 levels in *Inha*$^{-/-}$;*Smad3*$^{-/-}$ males compared with *Inha*$^{-/-}$ males. D, Comparison of serum testosterone levels between *Inha*$^{-/-}$;*Smad3*$^{-/-}$ (26 wk) and WT (10 wk) males. The following numbers of mice were used: activin A analysis, n = 5–8 for each group except the WT controls (n = 3); FSH, E_2, and testosterone assays, n = 4–6 for each group. Data are shown as mean ± SEM, and *bars without a common superscript* are significantly different at $P < 0.05$ (B, C, and D) or $P < 0.01$ (A).

Inha$^{-/-}$;*Smad3*$^{-/-}$ Males Have Highly Elevated FSH but Low E_2

Because FSH and E_2 have important implications in promoting tumor progression in *Inha* knockout mice (37, 38), serum levels of FSH and E_2 were determined in the double mutant mice. Despite the effects of loss of *Smad3* on the development of gonadal tumors and the observed cachexia-like syndrome, FSH levels remain highly elevated in the double-knockout males (10 wk: 45.42 ± 5.69 ng/ml; 26 wk: 47.57 ± 5.14 ng/ml) compared with the *Inha*$^{-/-}$ controls (25.67 ± 2.49 ng/ml; Fig. 3B; $P < 0.05$). The highly elevated FSH and markedly reduced tumorigenesis in the double-knockout males implicate SMAD3 in FSH-promoted tumor progression in the inhibin-deficient mice. In contrast to the FSH levels, serum E_2 was low in *Inha*$^{-/-}$;*Smad3*$^{-/-}$ males (10 wk: 16.05 ± 1.55 ng/ml; 26 wk: 29.85 ± 8.92 ng/ml) compared with *Inha*$^{-/-}$ males (135.95 ± 57.30 ng/ml; Fig. 3C; $P < 0.05$). Because the gonadal tumors in inhibin-deficient mice secrete E_2 (15), the reduced E_2 levels in the double-knockout males reflect the attenuation/absence of tumors. Serum testosterone was not significantly altered in the *Inha*$^{-/-}$;*Smad3*$^{-/-}$ males at the age of 26 wk compared with adult WT males (Fig. 3D; $P > 0.05$).

Up-Regulation of Testicular mRNA for Activin/Inhibin βB Subunit in the *Inha*$^{-/-}$ and *Inha*$^{-/-}$;*Smad3*$^{-/-}$ Males

Increased expression of activin βA subunit in the inhibin-deficient testicular tumors was previously demonstrated (45). This study addressed whether loss of

F, Liver weight from *Inha*$^{-/-}$ (7–11wk; n = 10) and *Inha*$^{-/-}$;*Smad3*$^{-/-}$ males (10 wk; n = 6 and 26 wk; n = 8). Note higher liver weight in the double-knockout males (10 wk and 26 wk) as compared with *Inha*$^{-/-}$ controls ($P < 0.05$). G, Hematocrits of *Inha*$^{-/-}$ (8–11 wk; n = 6) and *Inha*$^{-/-}$;*Smad3*$^{-/-}$ males (10 wk; n = 5 and 26 wk; n = 6). Note higher hematocrits in the double-knockout males (10 wk and 26 wk) as compared with *Inha*$^{-/-}$ controls ($P < 0.01$). Data are shown as mean ± SEM, and *bars without a common superscript* are significantly different. *Scale bars*, D and E, 50 μm; B and C, 100 μm.

inhibin would cause increased Activin/Inhibin βB subunit (*Inhbb*) expression in both tumor-free testis and testicular tumors. By using quantitative real-time PCR, we measured the mRNA expression for *Inhbb* in the testes of *Inha*$^{-/-}$ and *Inha*$^{-/-}$;*Smad3*$^{-/-}$ mice before tumor formation as well as in the testicular tumors from cachectic *Inha*$^{-/-}$ males at the advanced stage of tumor development (8–11 wk). The results showed that the testicular mRNA abundance for *Inhbb* in the 3-wk-old *Inha*$^{-/-}$ and *Inha*$^{-/-}$;*Smad3*$^{-/-}$ males was increased compared with the age-matched WT and *Smad3*$^{-/-}$ controls (Fig. 4A; $P < 0.05$). In the testicular tumors recovered from inhibin-deficient mice, *Inhbb* mRNA abundance was more than 10-fold higher than in the WT testes (Fig. 4B; $P < 0.01$), confirming tumors are active in activin production. The increased *Inhbb* in the testis of both *Inha* knockout and the double-knockout mice (before tumor formation), and the significantly reduced tumor development of the double-knockout males, further suggest that the potentiated activin signals cannot be adequately transduced in the absence of SMAD3, leading to the significantly attenuated gonadal tumor phenotype in the double-knockout males.

SMAD3 in Ovarian Tumor Development in Inhibin-Deficient Mice

We also examined an allelic series of *Inha* and *Smad3* mutant females and again found a difference in survival rate between the double homozygous and inhibin-deficient mice (Fig. 5A). Loss of one copy of *Smad3* (*Inha*$^{-/-}$;*Smad3*$^{+/-}$) caused a slightly rightward shift of the survival curve, whereas absence of *Smad3* in inhibin-deficient females resulted in 90% survival at 17 wk of age, a time at which 80% of *Inha*$^{-/-}$;*Smad3* WT and more than 65% of the *Inha*$^{-/-}$;*Smad3*$^{+/-}$ females died of the cachexia-like syndrome. However, this did not approximate the *Smad3*$^{-/-}$;*Inha* WT animals, which had a 100% survival by 26 wk of age.

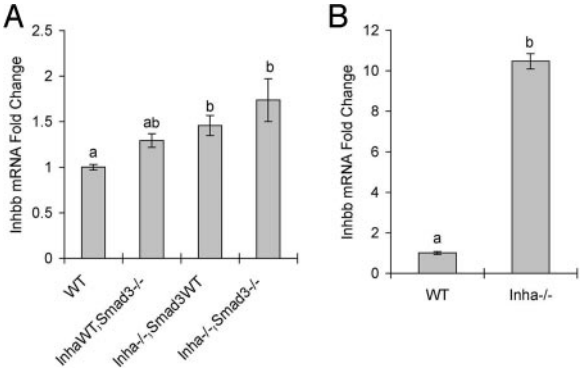

Fig. 4. Expression of the mRNA for *Inhbb* in Inhibin-Deficient Testes

A, Comparison of testicular Inhbb mRNA abundance among 21-d-old WT, *Smad3*$^{-/-}$, *Inha*$^{-/-}$, and *Inha*$^{-/-}$;*Smad3*$^{-/-}$ males (n = 3 for each genotype). Note that testicular mRNA abundance for Inhbb in the 3-wk-old *Inha*$^{-/-}$ and *Inha*$^{-/-}$;*Smad3*$^{-/-}$ males was increased compared with the age-matched WT and *Smad3*$^{-/-}$ controls ($P < 0.05$). B, Comparison of testicular Inhbb mRNA abundance between *Inha*$^{-/-}$ males with advanced tumors and adult WT males (n = 3–5 for each genotype). Note that the mRNA abundance for *Inhbb* in inhibin-deficient testicular tumors was more than 10-fold elevated compared with WT controls ($P < 0.01$). Fold changes in the relative mRNA expression of *Inhbb* in different genotypes relative to WT control were determined using ΔΔCT method. Data are shown as mean ± SEM, and *bars without a common superscript* are significantly different.

To analyze ovarian tumorigenesis, we first examined the double homozygous females at 6 (n = 1), 14 (n = 1), and 15 (n = 6) wk of age when cachexia was not evident. At 6 wk, no macro- and microscopic tumors were observed, but the ovaries had abnormal histology including oocyte degeneration (Fig. 5, B and C). At 14 and 15 wk of age, formation of small hemorrhagic cysts was observed in approximately 70% of the double-knockout females (Fig. 5, D and E). Histological analysis revealed the presence of premalignant lesions including tubule-like structures and degenerating oocytes (Fig. 5F) in addition to the cysts (Fig. 5E). However, multifocal and hemorrhagic tumors developed as early as 16 wk of age in one of the 12 double-knockout females that were designated for the 26-wk period study. Advanced tumors were recovered from the majority of cachectic *Inha*$^{-/-}$;*Smad3*$^{-/-}$ females beyond 17 wk of age that had histological characteristics indistinguishable from those observed in *Inha*$^{-/-}$ mice (Fig. 5, G and H). At the final time point of 26 wk, there were two double-knockout females that had not developed gonadal tumors.

Despite the delayed tumor progression in the double-knockout females, the above histological evidence (Fig. 5, B and C) indicated ovarian defects in these females. To further examine whether ovulation is possible to occur in *Inha* and *Smad3* double knockouts, a superovulation experiment was performed using 3- to 4-wk-old females. Ovulation in the WT controls was efficiently elicited by exogenous gonadotropins with an average of 47.8 ± 2.1 oocytes per mouse (n = 5). In contrast, no oocytes were recovered from the double-knockout females (n = 3).

Loss of SMAD3 in Inhibin-Deficient Females Delays the Development of the Cachexia-Like Wasting Syndrome

The effects of SMAD3 deficiency on the development of the cachexia-like syndrome were also examined in females. Although the wasting syndrome still occurred in most of the *Inha*$^{-/-}$;*Smad3*$^{-/-}$ females during the examined time period, the process is delayed compared with inhibin-deficient mice that suffered from a severe early weight loss (Fig. 6A). The weight curve of *Smad3*$^{-/-}$ females was characterized by a continuous weight gain during the 26-wk period (Fig. 6A). To address the effect of *Smad3* loss of function on the

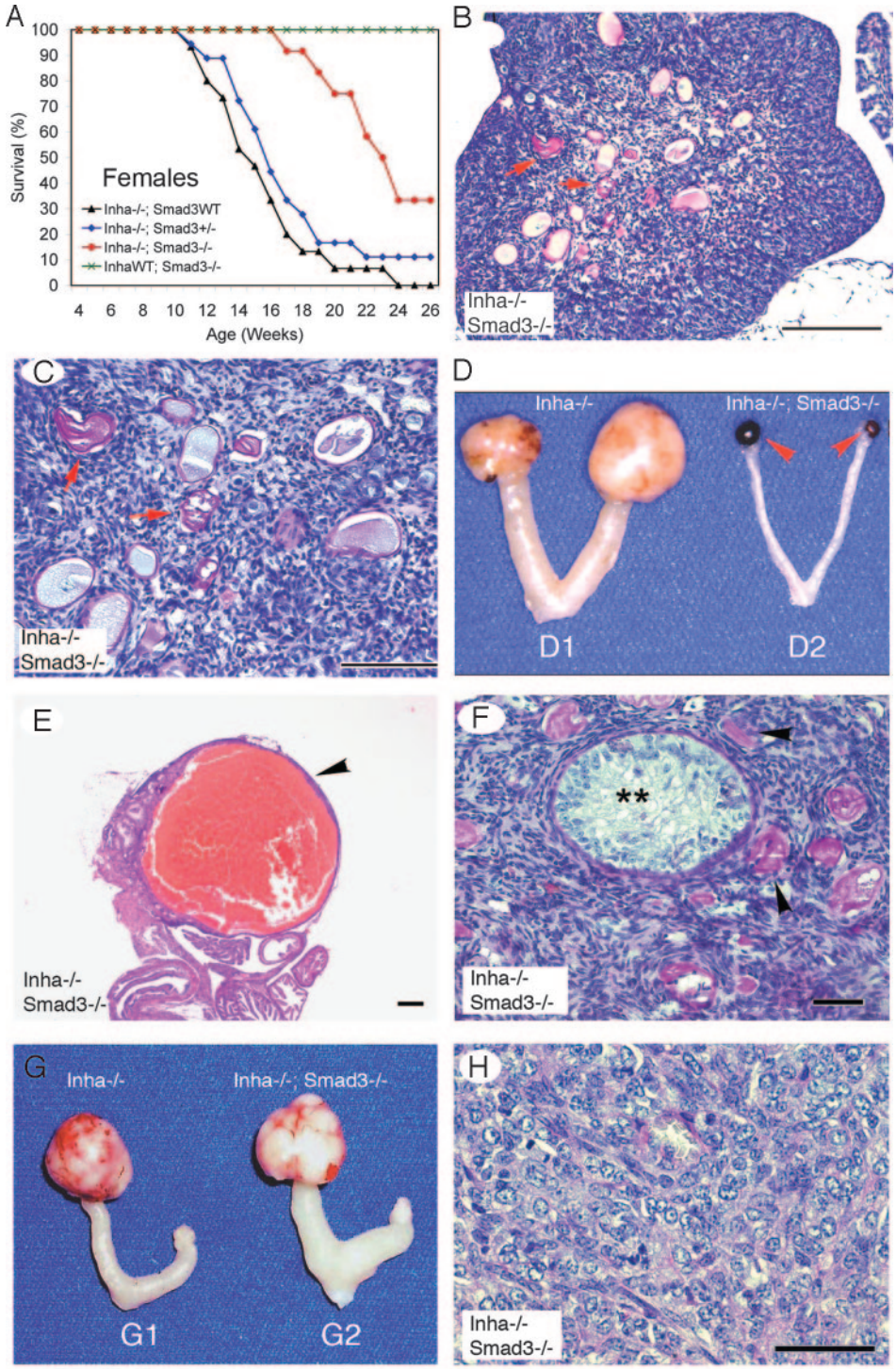

Fig. 5. Ovarian Tumor Development in *Inha* and *Smad3* Double Homozygous Females

A, Survival curve of *Inha*$^{-/-}$ (n = 15), *Inha*$^{-/-}$;*Smad3*$^{+/-}$ (n = 18), *Inha*$^{-/-}$;*Smad3*$^{-/-}$ (n = 12), and *Inha* WT;*Smad3*$^{-/-}$ (n = 10) females. B and C, Ovarian histology of a 6-wk-old *Inha*$^{-/-}$;*Smad3*$^{-/-}$ female. Note that although no obvious tumors are present in the ovary, follicle development was altered and oocytes degenerated. D, Ovarian tumors from a 12-wk-old *Inha*$^{-/-}$ female (D1) were grossly large and hemorrhagic, whereas formation of small hemorrhagic cysts (*arrowheads*) instead of tumors was observed in a 14-wk-old double-knockout female (D2). E and F, Representative histology of ovaries from a 14-wk-old double-knockout female (D2) depicting the hemorrhagic cyst (E; *arrowhead*), tubule-like structures (F; **) and zona pelucida (ZP) remnants (F; *arrowheads*). G, Unilateral ovarian tumors from a 15-wk-old *Inha*$^{-/-}$ female (G1) and a 26-wk-old *Inha*$^{-/-}$;*Smad3*$^{-/-}$ female (G2), respectively. Tumors from both genotypes were hemorrhagic and grossly indistinguishable. H, Representative histology of the ovarian tumor from a 26-wk-old double-knockout female (G2). *Scale bars*, F and H, 50 μm; C, 100 μm; B and E, 200 μm.

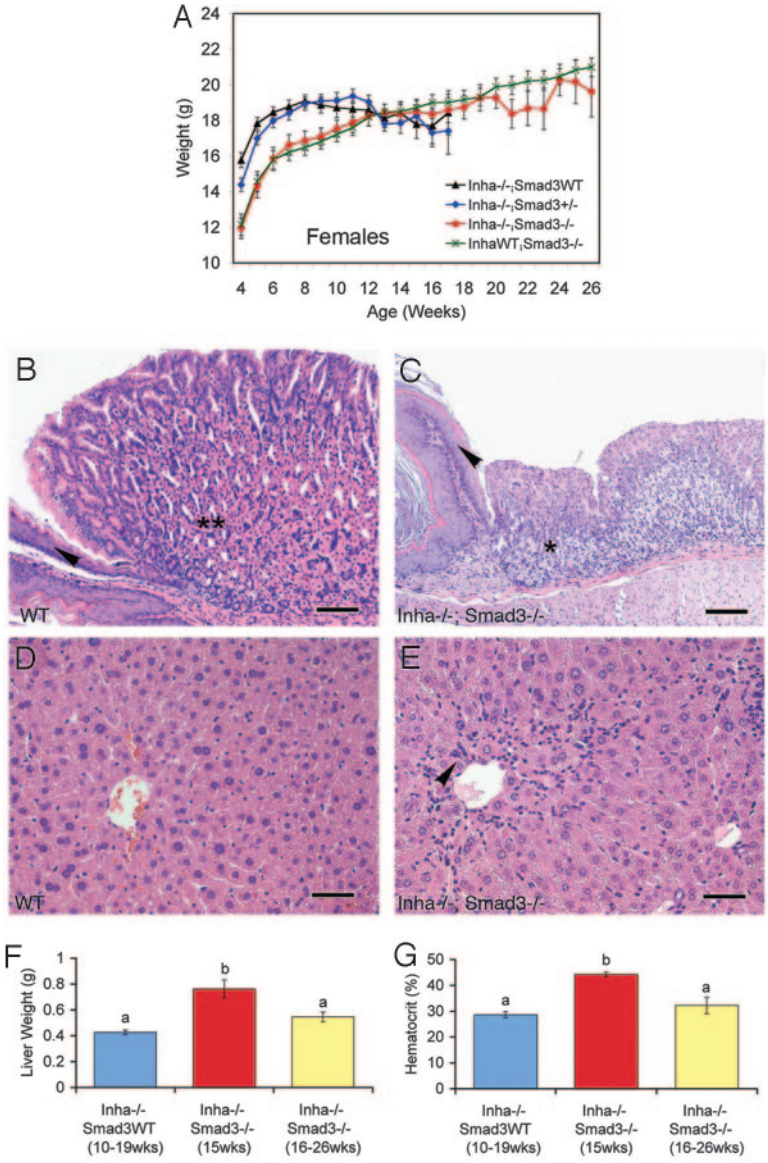

Fig. 6. Development of the Cachexia-Like Syndrome in *Inha*$^{-/-}$;*Smad3*$^{-/-}$ Females

A, The weight curves of *Inha*$^{-/-}$ (n = 15), *Inha*$^{-/-}$;*Smad3*$^{+/-}$ (n = 18), *Inha*$^{-/-}$;*Smad3*$^{-/-}$ (n = 12), and *Inha* WT;*Smad3*$^{-/-}$ (n = 10) females. B and C, Glandular stomachs from a 15-wk-old WT female (B) and a 26-wk-old cachectic *Inha*$^{-/-}$; *Smad3*$^{-/-}$ female with advanced tumors (C). Note the depletion of parietal cells in the double-knockout female. The orientation of the pictures is the same as described in Fig. 2. D and E, Histology of livers from a 15-wk-old WT female (D) and a 22-wk-old *Inha*$^{-/-}$;*Smad3*$^{-/-}$ female with advanced tumors (E). Note the hepatocellular death around the central vein and lymphocytic infiltration (*arrowhead*) in the livers of the double-knockout female. F, Liver weight from *Inha*$^{-/-}$ (10–19 wk; n = 14) and *Inha*$^{-/-}$;*Smad3*$^{-/-}$ females (15 wk; n = 6 and 16–26 wk; n = 7). Note the comparable liver weight between the cachectic double-knockout and *Inha*$^{-/-}$ females at the advanced stage of tumor development. G, Hematocrits of *Inha*$^{-/-}$ (10–19 wk; n = 9) and *Inha*$^{-/-}$;*Smad3*$^{-/-}$ females (15 wk; n = 5 and 16–26 wk; n = 5). Note the comparable hematocrits between the double-knockout and *Inha*$^{-/-}$ females at the advanced tumor stages. Data are shown as mean ± SEM, and *bars without a common superscript* are significantly different at $P < 0.01$. *Scale bars*, D and E, 50 μm; B and C, 100 μm.

development of the wasting syndrome in inhibin-deficient females, female *Inha*$^{-/-}$;*Smad3*$^{-/-}$ mice were killed at an early time point (15 wk) when cachexia was not apparent in the double knockouts, a point at which the majority of *Inha*$^{-/-}$ females suffered from weight loss. Histological analysis revealed that the pathological characteristics of inhibin-deficient mice in the stomach and liver were not found in the 15-wk-old non-cachectic double mutants (data not shown) but were evident in the *Inha*$^{-/-}$;*Smad3*$^{-/-}$ females at the advanced tumor stage (Fig. 6, B–E). Furthermore, the liver weight (Fig. 7F) and hematocrits (Fig. 6G) in the 15-wk-old double mutants were higher compared with those in the *Inha*$^{-/-}$ females ($P < 0.01$). However, at

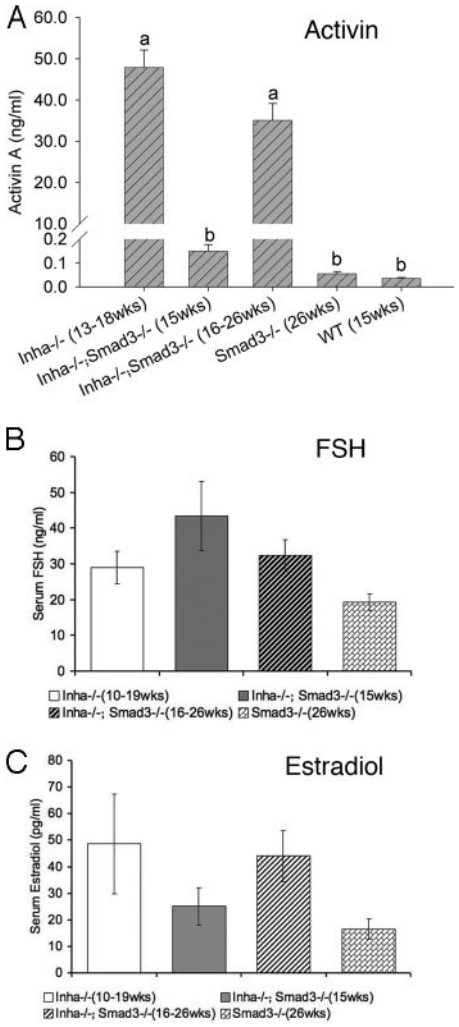

Fig. 7. Serum Activin A, FSH, and E_2 Levels in the *Inha*$^{-/-}$;*Smad3*$^{-/-}$ Female Mice

A, Comparison of serum activin A levels among *Inha*$^{-/-}$, *Inha*$^{-/-}$;*Smad3*$^{-/-}$ (15 wk and 16–26 wk), *Smad3*$^{-/-}$, and WT females (n = 3–6 for each group). Note the significantly lower activin A levels in the noncachectic *Inha*$^{-/-}$;*Smad3*$^{-/-}$ females (15 wk) which have no tumors compared with the *Inha*$^{-/-}$ mice. Activin A levels were dramatically elevated in the cachectic double-knockout females (16–26 wk) with advanced tumors compared with the noncachectic *Inha*$^{-/-}$;*Smad3*$^{-/-}$ (15 wk), *Smad3*$^{-/-}$, and WT females. B, Comparison of serum FSH levels among *Inha*$^{-/-}$, *Inha*$^{-/-}$;*Smad3*$^{-/-}$ (10 wk and 26 wk), and *Smad3*$^{-/-}$ mice (n = 4–10 for each genotype). Note that comparable levels of FSH in the females were found between *Inha*$^{-/-}$ and the cachectic double-knockout mice. C, Comparison of serum E_2 levels among *Inha*$^{-/-}$, *Inha*$^{-/-}$;*Smad3*$^{-/-}$, and *Smad3*$^{-/-}$ mice. Note the comparable serum E_2 levels between *Inha*$^{-/-}$ mice and the cachectic double knockouts at the advanced tumor stages. Data are shown as mean ± SEM, and *bars without a common superscript* are significantly different at $P < 0.01$.

later stages when the cachexia was evident in the double-knockout females, reduction of liver weight and anemia were detected (Fig. 6, F and G).

Activin A levels (Fig. 7A) were also analyzed to determine the correlation of activins with cachexia and gonadal tumor progression in females. Two groups of double-knockout females were examined in this study, double knockouts at the advanced tumor stage (16–26 wk) and at 15 wk of age (15 wk; no tumors were formed in these mice), to test the following hypotheses: 1) the double-knockout female mice with cachexia and advanced tumors (16- to 26-wk group) would have similarly high levels of serum activins as *Inha* null mice that had advanced tumors; and 2) double-knockout females at an earlier age (15 wk) when tumors and cachexia were not visible in the vast majority of them would have lower serum activin levels in comparison with cachectic *Inha* null mice at a similar age. Concordant with the cachexia symptoms and tumor status, the cachectic double-knockout females that developed advanced tumors had markedly elevated serum activin A levels (35.06 ± 4.10 ng/ml) compared with 15-wk-old WT controls (0.04 ± 0.00 ng/ml) as well as 15-wk-old *Inha*$^{-/-}$;*Smad3*$^{-/-}$ and 26-wk-old *Smad3*$^{-/-}$ females (0.05 ± 0.01 ng/ml; $P <$ 0.01). However, circulating activin A levels were significantly lower in the 15-wk-old double-knockout mutants (0.15 ± 0.03 ng/ml) compared with the *Inha*$^{-/-}$ females (47.87 ± 4.23 ng/ml; $P < 0.01$).

FSH and E_2 Levels in *Inha*$^{-/-}$;*Smad3*$^{-/-}$ Females

FSH levels were not significantly different between the double-knockout and *Inha*$^{-/-}$ female mice (Fig. 7B; $P > 0.05$). Comparable serum E_2 levels were observed between the cachectic double knockouts and the *Inha*$^{-/-}$ controls at the terminal stages of tumor development (Fig. 7C, $P > 0.05$). However, E_2 levels in the 15-wk-old double-knockout females (25.20 ± 7.06 ng/ml) were lower than those in the *Inha*$^{-/-}$ mice (48.70 ± 18.75 ng/ml) although statistical significance was not achieved (Fig. 7C; $P > 0.05$).

DISCUSSION

Inhibin was originally identified based upon its properties of inhibiting production of FSH. We examined the endogenous role of inhibin by generating inhibin mutant mice (14). Inhibin-deficient mice developed sex cord-stromal tumors and a severe cachexia-like wasting syndrome (14, 15). Such gonadal tumors afflict humans, and mouse models can be exploited to help provide rational approaches to therapies. Inhibin is an antagonist of activin, which signals via SMAD2 and SMAD3. We undertook the current studies to dissect the relative roles of SMAD2 and SMAD3 in gonadal tumorigenesis and associated cachexia. The current studies demonstrated that *Inha* and *Smad3* double homozygous males had substantially extended life span compared with *Inha* null male mice. Further, the double homozygous males were protected from early

tumorigenesis and the severe weight loss. Virtually 100% of inhibin-deficient males develop bilateral, large, aggressive hemorrhagic testicular cancers. In contrast, the double mutant mice either did not have testicular tumors or when they did occur, they were typically a unilateral, slow-growing mild form of the disease. Furthermore, loss of *Smad3* in inhibin-deficient males partially rescued the fertility. SMAD3 deficiency also reduced female ovarian tumorigenesis but to a much milder degree than in males. Although delayed compared with controls, the majority of double-knockout females developed ovarian tumors by 26 wk. This suggests that genes in addition to *Smad3* have important roles in female inhibin-deficient gonadal tumorigenesis. These data highlight the complex role that SMAD3 signaling plays in carcinogenesis; loss of *Smad3* promotes intestinal and inhibits gonadal tumorigenesis. Although the mechanism contributing to the effect of loss of *Smad3* in tumorigenesis in the intestine and gonads remains unclear, it seems that the differences in cellular origin-related transcription factors and coregulators may account significantly for the contrasting roles of SMAD3 in tumorigenesis in these organs. Further, these results enhance our understanding of the roles of activins in gonadal tumor development. Of note, although significant effects of loss of *Smad3* were found in the inhibin-deficient mice, no discernible impact of inhibin deficiency on the *Smad3*-related colorectal tumor phenotype was observed. In fact, one might expect the result. Whereas loss of activin signaling through SMAD3 results in cancer in the colon (*i.e*. SMAD3 is a tumor suppressor in the colon), increased activin signaling through SMAD3 (and/or SMAD2) in the gonads promotes sex cord-stromal tumors (*i.e.* SMAD3 is functioning like an oncogene). Furthermore, because SMAD3 in the colon is downstream of activin signaling, the effects of absence of inhibin and relative levels of activin are inconsequential because the key transcriptional signaling protein (*i.e*. SMAD3) is absent.

It is possible that double-knockout males will develop enhanced gonadal tumors beyond 26 wk, the time-point at which we did our final analyses. However, longer term analyses were expected to be compromised by the development of colorectal cancer in *Smad3* null mice. In our study, colorectal cancers became evident in the double-knockout mice or *Smad3* null mice at 21 wk of age at only a low incidence; therefore, 26 wk was set as the end point of this study as colonic carcinogenesis is progressive and may have hindered studies beyond that time.

Coincident with the significantly reduced tumor development, the fertility of double-knockout males was partially rescued during a 3-month test period, further suggesting that the infertility observed in inhibin-deficient mice was secondary to gonadal tumor development. Results from this study support our earlier findings that inhibin is not essential for testicular development, spermatogenesis, and male reproductive potential (16). Unlike *Inha* null males, female mice deficient in inhibin are never fertile (16). Even under pharmacological conditions, there appeared to be a block in folliculogenesis and/or oogenesis in these females (3–4 wk) before tumor developed (16). Moreover, although *Smad3* null males demonstrate normal fertility, *Smad3* null females are subfertile in our colony. In an attempt to assess the reproductive efficacy of the *Inha* and *Smad3* double-knockout females, we evaluated the histology of 6-wk-old double-knockout females, and significant ovarian defects including oocyte degeneration and lack of normal developing follicles were found. Pharmacological superovulation of the double-knockout females that had no tumors resulted in an absence of oocytes, confirming an ovulation defect in mice lacking inhibin and *Smad3*. The above evidence suggests that the double-knockout females would be expected to be infertile or have dramatically compromised fertility. The mechanism of fertility defects in the inhibin-deficient females remains to be established in our future studies.

Activins have several important embryogenic functions including murine craniofacial development (23), and germ layer specification in frogs and fish (46, 47). In addition, several studies suggest that activins also regulate growth and survival (10). A direct link between activins and tumor development has not yet been established (4). However, several lines of evidence highlight the potential importance of activins in tumor growth and progression. First, *in vitro* evidence demonstrated that activins can stimulate the proliferation and incorporation of thymidine into DNA of gonadal tumor cell lines derived from inhibin and p53-deficient mice (39). Second, the activin signaling is potentiated in inhibin-deficient mice, which is supported by the following evidence. The overexpression of activin/inhibin subunits was observed in ovarian and testicular tumors (4). We previously demonstrated that activin βA subunit in the inhibin-deficient testes was dramatically increased (45), and the current study provided further evidence that testicular activin βB mRNA is increased in inhibin-deficient mice before tumor formation and further elevated in the testicular tumors. Moreover, *Inha* knockout mice have elevated FSH levels (14), and FSH was reported to regulate *Smad3* mRNA in rat testis (48). We recently found that *Smad3* mRNA abundance is 2-fold increased in the testicular tumors of inhibin-deficient mice compared with WT testis (Li, Q., and M. M. Matzuk, unpublished observation). Third, transgenic expression of follistatin, a proposed activin antagonist (49), reduced tumorigenic process and prolonged the life span of inhibin mutant mice (50). In addition, mice deficient in inhibin and FSH have markedly reduced activins and develop slow-growing tumors (37). However, mice deficient in both inhibin and ActRII still develop gonadal sex cord-stromal tumors (17). It is possible that this is due to activin signaling

through ActRIIB that is present in the ovary and testis (51, 52) or other unidentified receptor(s). The involvement of activin signaling in tumorigenesis was further corroborated by the finding that administration of ActRII-mFc, an activin antagonist, significantly delayed gonadal tumor progression in inhibin-deficient mice (67). In support of the above findings, the current studies demonstrated that loss of activin-responsive SMAD3 in inhibin-deficient mice dramatically reduced gonadal tumor development. However, SMAD3 also transduces other signals, such as TGF-β. Furthermore, our results indicate that SMAD3 is the predominant, albeit not the only, activin-responsive SMAD in the testis (43, 44), whereas both SMAD2 and SMAD3 are required in the ovary downstream of activin signaling cascades. Interestingly, significant changes of gonadal *Smad2* mRNA abundance in the double-knockout mice were not found (Li, Q., and M. M. Matzuk, unpublished observation).

Because gonadal tumors in inhibin-deficient mice occur as focal lesions, secondary event(s) or genetic modifiers should exist to fulfill the malignant transformation. To define the mechanisms of gonadal tumorigenesis, genetic engineering has been applied, and a number of genetically modified mouse lines have been created and used in our previous studies. The genetic modifiers identified in our former studies include GnRH (53), FSH (37), anti-Mullerian hormone (54) and its receptor (55), follistatin (50), androgen receptor (56), cyclin D2 (57), p27 (58), and estrogen receptors (38). Among these modifiers, FSH is an important trophic modifier factor for gonadal tumorigenesis via influencing the tumor progression in inhibin-deficient mice (37). Moreover, estrogen receptors (*ER*α and *ER*β) and *Inha* triple-knockout mouse models suggest that estrogen signaling plays a critical role in promoting tumor progression in males (38). Therefore, it was interesting to determine FSH and E_2 levels in *Inha* and *Smad3* double-knockout mice. Despite the pronounced effects of loss of *Smad3* on gonadal tumorigenesis, FSH levels in the double homozygous males were even higher than those in inhibin-deficient mice. The reason why loss of *Smad3* in the inhibin-deficient background resulted in even higher serum FSH in the males is not clear. However, it seems that serum E_2 plays at least a partial role. It is interesting to note that E_2 levels in the double-knockout males at both 10 and 26 wk of age were lower than those in the inhibin-deficient mice, which clearly correlated with the reduced tumor progression in these double-knockout mice. As opposed to the high E_2 levels in inhibin-deficient mice, we created a low E_2 environment in the circulation of inhibin-deficient males, which did not develop or developed slow-growing tumors when functional deletion of *Smad3* was introduced. It is possible that the low level of E_2 may further contribute to the elevation of FSH in the serum via a negative feedback mechanism (59). Considering the role of FSH in gonadal tumor formation and progression (37) as well as FSH regulation of testicular *Smad3* (48), it is possible that SMAD3 is involved in FSH-promoted tumor progression. However, the possibility cannot be excluded that other TGF β ligands might signal through SMAD3 to regulate FSH levels.

The development of the wasting syndrome in inhibin-deficient mice is mediated by activin signaling through ActRII in the liver and glandular stomach, which confers the pathological changes and nutritional defects described previously (15, 17). In agreement with the roles of activins in the liver (60, 61) and the effects of recombinant activin A on hepatocellular death both *in vivo* and *in vitro* (62), *ActRII* mRNA is detectable in the liver and stomach (17). Therefore, loss of *ActRII* in the inhibin-deficient mice led to the histologically normal liver and stomach and consequently forestalled the weight loss in the double-knockout mice (17). The current studies strengthened the notion that the development of cachexia-like syndrome is secondary to tumor formation and elevation of serum activin levels. Activin levels correlated well with tumor status in the current studies. In the $Inha^{-/-}$;$Smad3^{-/-}$ males, the absence of secondary pathological lesions in the liver and stomach reflected the low activin A levels found in these double-knockout males even at 26 wk. In contrast, the majority of double-knockout females developed advanced tumors by 26 wk, and these cachectic mice had similarly elevated circulating activin A levels as the inhibin-deficient mice, as well as pathological lesions in the stomach and liver. Based on the primary role of activins in inducing cachexia symptoms in inhibin-deficient mice of both sexes (17) and cachexia symptoms observed in the majority of female double-knockout mice at the advanced stage of tumor progression, it appears that both SMAD2 and SMAD3 or SMAD2 alone are/is required for activin signaling in the liver and stomach to confer the pathological lesions.

The current findings, combined with our previous genetic studies, strongly indicate that SMAD3 acts as the dominant SMAD in the testis whereas both SMAD2 and SMAD3 appear to be required in the ovary for activin signaling cascades. These results illustrate the differences between males and females in the role of SMAD3 in gonadal tumorigenesis. Moreover, our findings suggest that the activin-induced cachexia syndrome is potentially mediated through SMAD2 and SMAD3 or only through SMAD2 in the stomach and liver. Elucidation of the functional redundancy of SMAD2 and SMAD3 in mediating tumorigenesis depends on the generation of *Smad2*, *Smad3,* and *Inha* triple knockouts in the testis and ovary. Furthermore, identification of the target genes downstream of the SMAD2/SMAD3 signaling pathways that confer tumorigenesis remains one of our future goals.

MATERIALS AND METHODS

Generation and Genotyping of *Inha* and *Smad3* Compound Mutant Mice

All mice lines used in this experiment were maintained on a mixed C57BL/6/129S6/SvEv genetic background and handled according to the NIH Guide for the Care and Use of Laboratory Animals. Generation of inhibin-deficient mice (14) and *Smad3* mutant mice (35) has been previously described. To generate double mutant mice deficient in inhibin and SMAD3, $Inha^{+/-}$ mice were mated to $Smad3^{+/-}$ mice to produce double heterozygous mice ($Inha^{+/-}$;$Smad3^{+/-}$). The double heterozygous mice were then interbred and double-knockout mice ($Inha^{-/-}$;$Smad3^{-/-}$) were obtained from the offspring. The $Inha^{-/-}$;$Smad3^{-/-}$ mice were obtained at the expected mendelian ratio of 1:16 with similar numbers of males and females. To facilitate the generation of $Inha^{-/-}$;$Smad3^{-/-}$ mice, the double heterozygous females were bred to the double homozygous males to increase the frequency of double homozygous mice to 1:4.

Genomic tail DNA was used for the genotype analysis. Genotyping of *Inha* mutant mice was conducted by Southern blot using ^{32}P-labeled probes (14) or PCR using primers (primer 1: 5′-CCT GGG TGG CGC AGG ATA TGG-3′; primer 2: 5′-GGT CTC CTG CGG CTT TGC GC-3′; and primer 3: 5′-GGA TAT GCC CTT GAC TAT AAT G-3′) to identify WT (primer 1+ primer 2) or *Inha* mutant allele (primer 1+ primer 3). Genotyping of *Smad3* WT (primer A + primer B) and null (primer A + primer C) allele was performed using PCR with the following primers including primer A: 5′-TGG ACT TAG GAG ACG GCA GTC C-3′; primer B: 5′-CTT CTG AGA CCC TCC TGA GTA GG-3′; and primer C: 5′-CTC TAG AGC GGC CTA CGT TTG G-3′.

Weights and Survival Data

Body weights of the mice were measured and recorded once a week at 1630–1800 h every Wednesday for a period of 4–26 wk. The development of cachexia symptoms including weight loss, kyphoscoliosis, sunken eye, *etc*., was monitored (15). The mice were counted weekly and killed when overt signs of cachexia wasting symptoms developed.

Histological Analysis

Ovary, testis, liver, and stomach were collected from mice at the time of euthanasia and fixed in 10% (vol/vol) neutral buffered formalin overnight. Samples were then transferred to 70% ethanol before being embedded and sectioned for hematoxylin and eosin (liver, stomach, and some ovary and testis samples) or periodic acid Schiff-hematoxylin (ovary and testis) staining using standard procedures in the Pathology Core Services Facility at Baylor College of Medicine.

Superovulation Experiment

Three to 4-wk-old *Inha* and *Smad3* double-knockout females or WT controls were ip injected with pregnant mare serum gonadotropin (5 IU/mouse) and followed by an ip injection of human chorionic gonadotropin (5 IU/mouse; ip) 48 h later. The next morning, the cumulus oocyte complexes were surgically recovered from the oviduct, and the oocytes were counted after the cumulus cells were removed by enzymatic treatment.

Hematocrit Analysis

Periorbital blood was collected from isoflurane-anesthetized mice into heparinized microhematocrit capillary tubes (Baxter Healthcare Corp., Deerfield, IL). The blood was spun for 15 min in a microhematocrit centrifuge, and the hematocrit was read on a microcapillary reader and recorded.

Hormone Analyses

Blood samples were collected from mice anesthetized with isoflurane inhalation into serum separator tubes (Becton Dickinson, Franklin Lakes, NJ) by cardiac puncture at the time of euthanasia. Blood was allowed to clot at room temperature, and serum was then separated by centrifugation and kept at −20 C. Total activin A was measured using a specific ELISA (63) according to the manufacturer's instructions (Oxford Bio-Innovations, Oxfordshire, UK) with modifications (64). The average intraplate coefficient of variation (CV) was 9.0% and the interplate CV was 8.6% (n = 4 plates). The limit of detection was 0.01 ng/ml. Serum FSH, E_2, and testosterone were analyzed by the Ligand Assay and Analysis Core at the Center for Research in Reproduction, University of Virginia. The limit of detection for FSH and E_2 was 2 ng/ml and 10 pg/ml, respectively. The limit of detection for testosterone was 10 ng/dl (detailed information regarding the method including antibodies used is available at http://www.healthsystem.virginia.edu/internet/crr/ligand.cfm).

RNA Isolation and Quantitative Real-Time RT-PCR

Total RNA was isolated from testes using RNeasy Mini Kit (QIAGEN, Inc., Valencia, CA) according to the manufacturer's instructions. Two hundred nanograms of total RNA was reverse transcribed using Superscript III reverse transcriptase (Invitrogen, Carlsbad, CA) and oligo$(dT)_{12–18}$ primers (Invitrogen) in a 20- μl reaction system. Real-time PCR was performed as previously described (65) using the ABI Prism 7500 Sequence Detection System (Applied Biosystems, Foster City, CA) with a program consisting of 40 cycles of 95 C for 15 sec and 60 C for 1 min. Briefly, Taqman assay (*Inhbb*, Mm01286587) was performed in 20 μl reaction volume using the TaqMan Universal PCR Master Mix (ABI). The reactions were set up in duplicate in a 96-well plate (ABI). Expression of *Inhbb* was normalized relative to that of the endogenous control (*Gapdh*) mRNA and $\Delta\Delta$CT method was used for the calculation (66). Negative controls of reverse transcription reactions in which reverse transcriptase was omitted from reactions were included in the analysis to monitor potential genomic DNA contamination.

Statistical Analysis

Differences among groups were assessed by ANOVA, and the mean between individual groups was further compared using Tukey's test. Data were reported as mean ± SEM, and $P < 0.05$ was considered to be statistically significant.

Acknowledgments

Ankur Nagaraja provided testicular tumor RNA for the quantitative PCR experiment. We thank Dr. Stephanie Pangas for critical review of the manuscript.

Received March 19, 2007. Accepted June 21, 2007.

Address all correspondence and requests for reprints to: Martin M. Matzuk, M.D., Ph.D., Stuart A. Wallace Chair and Professor, Department of Pathology, One Baylor Plaza, Baylor College of Medicine, Houston, Texas 77030. E-mail: mmatzuk@bcm.tmc.edu.

This work was supported by National Institutes of Health Grants HD32067 and CA60651 (to M.M.M.) and National

Health and Medical Research Council Grants 384108 and 334011 (to K.L.L.). Serum FSH and testosterone analyses, performed at the University of Virginia Center for Research in Reproduction Ligand Assay and Analysis Core, were supported by National Institute of Child Health and Human Development (SCCPRR) Grant U54-HD28934.

Disclosure Statement: The authors have no disclosures of conflict of interest.

REFERENCES

1. Chang H, Brown CW, Matzuk MM 2002 Genetic analysis of the mammalian transforming growth factor-β superfamily. Endocr Rev 23:787–823
2. Massague J 1998 TGF-β signal transduction. Annu Rev Biochem 67:753–791
3. Massague J 2000 How cells read TGF-β signals. Nat Rev Mol Cell Biol 1:169–178
4. Risbridger GP, Schmitt JF, Robertson DM 2001 Activins and inhibins in endocrine and other tumors. Endocr Rev 22:836–858
5. Xu J, McKeehan K, Matsuzaki K, McKeehan WL 1995 Inhibin antagonizes inhibition of liver cell growth by activin by a dominant-negative mechanism. J Biol Chem 270:6308–6313
6. Bilezikjian LM, Blount AL, Donaldson CJ, Vale WW 2006 Pituitary actions of ligands of the TGF-β family: activins and inhibins. Reproduction 132:207–215
7. Findlay JK, Drummond AE, Dyson M, Baillie AJ, Robertson DM, Ethier JF 2001 Production and actions of inhibin and activin during folliculogenesis in the rat. Mol Cell Endocrinol 180:139–144
8. Yan W, Burns KH, Matzuk MM 2003 Genetic engineering to study testicular tumorigenesis. APMIS 111:174–181; discussion 182–183
9. Pangas SA, Woodruff TK 2000 Activin signal transduction pathways. Trends Endocrinol Metab 11:309–314
10. Brown CW, Li L, Houston-Hawkins DE, Matzuk MM 2003 Activins are critical modulators of growth and survival. Mol Endocrinol 17:2404–2417
11. Bristol-Gould SK, Kreeger PK, Selkirk CG, Kilen SM, Cook RW, Kipp JL, Shea LD, Mayo KE, Woodruff TK 2006 Postnatal regulation of germ cells by activin: the establishment of the initial follicle pool. Dev Biol 298: 132–148
12. Phillips DJ, Woodruff TK 2004 Inhibin: actions and signalling. Growth Factors 22:13–18
13. Loveland KL, Robertson DM 2005 The TGFb superfamily in Sertoli cell biology. In: Griswold M, Skinner M, eds. Sertoli cell biology. New York: Elsevier Science; 227–247
14. Matzuk MM, Finegold MJ, Su JG, Hsueh AJ, Bradley A 1992 α-Inhibin is a tumour-suppressor gene with gonadal specificity in mice. Nature 360:313–319
15. Matzuk MM, Finegold MJ, Mather JP, Krummen L, Lu H, Bradley A 1994 Development of cancer cachexia-like syndrome and adrenal tumors in inhibin-deficient mice. Proc Natl Acad Sci USA 91:8817–8821
16. Matzuk MM, Kumar TR, Shou W, Coerver KA, Lau AL, Behringer RR, Finegold MJ 1996 Transgenic models to study the roles of inhibins and activins in reproduction, oncogenesis, and development. Recent Prog Horm Res 51:123–154; discussion 155–157
17. Coerver KA, Woodruff TK, Finegold MJ, Mather J, Bradley A, Matzuk MM 1996 Activin signaling through activin receptor type II causes the cachexia-like symptoms in inhibin-deficient mice. Mol Endocrinol 10:534–543
18. Derynck R, Zhang YE 2003 Smad-dependent and Smad-independent pathways in TGF-β family signalling. Nature 425:577–584
19. Massague J 1992 Receptors for the TGF-β family. Cell 69:1067–1070
20. Mathews LS, Vale WW 1991 Expression cloning of an activin receptor, a predicted transmembrane serine kinase. Cell 65:973–982
21. Attisano L, Carcamo J, Ventura F, Weis FM, Massague J, Wrana JL 1993 Identification of human activin and TGF β type I receptors that form heteromeric kinase complexes with type II receptors. Cell 75:671–680
22. Mathews LS 1994 Activin receptors and cellular signaling by the receptor serine kinase family. Endocr Rev 15: 310–325
23. Matzuk MM, Kumar TR, Vassalli A, Bickenbach JR, Roop DR, Jaenisch R, Bradley A 1995 Functional analysis of activins during mammalian development. Nature 374: 354–356
24. Mehra A, Wrana JL 2002 TGF-β and the Smad signal transduction pathway. Biochem Cell Biol 80:605–622
25. Moustakas A, Souchelnytskyi S, Heldin CH 2001 Smad regulation in TGF-β signal transduction. J Cell Sci 114: 4359–4369
26. Massague J, Blain SW, Lo RS 2000 TGFβ signaling in growth control, cancer, and heritable disorders. Cell 103: 295–309
27. ten Dijke P, Hill CS 2004 New insights into TGF-β-Smad signalling. Trends Biochem Sci 29:265–273
28. Suszko MI, Lo DJ, Suh H, Camper SA, Woodruff TK 2003 Regulation of the rat follicle-stimulating hormone β-subunit promoter by activin. Mol Endocrinol 17:318–332
29. Bernard DJ 2004 Both SMAD2 and SMAD3 mediate activin-stimulated expression of the follicle-stimulating hormone β subunit in mouse gonadotrope cells. Mol Endocrinol 18:606–623
30. Hamamoto T, Beppu H, Okada H, Kawabata M, Kitamura T, Miyazono K, Kato M 2002 Compound disruption of smad2 accelerates malignant progression of intestinal tumors in apc knockout mice. Cancer Res 62:5955–5961
31. Heyer J, Escalante-Alcalde D, Lia M, Boettinger E, Edelmann W, Stewart CL, Kucherlapati R 1999 Postgastrulation Smad2-deficient embryos show defects in embryo turning and anterior morphogenesis. Proc Natl Acad Sci USA 96:12595–12600
32. Nomura M, Li E 1998 Smad2 role in mesoderm formation, left-right patterning and craniofacial development. Nature 393:786–790
33. Waldrip WR, Bikoff EK, Hoodless PA, Wrana JL, Robertson EJ 1998 Smad2 signaling in extraembryonic tissues determines anterior-posterior polarity of the early mouse embryo. Cell 92:797–808
34. Weinstein M, Yang X, Li C, Xu X, Gotay J, Deng CX 1998 Failure of egg cylinder elongation and mesoderm induction in mouse embryos lacking the tumor suppressor smad2. Proc Natl Acad Sci USA 95:9378–9383
35. Zhu Y, Richardson JA, Parada LF, Graff JM 1998 Smad3 mutant mice develop metastatic colorectal cancer. Cell 94:703–714
36. Yang X, Letterio JJ, Lechleider RJ, Chen L, Hayman R, Gu H, Roberts AB, Deng C 1999 Targeted disruption of SMAD3 results in impaired mucosal immunity and diminished T cell responsiveness to TGF-β. EMBO J 18: 1280–1291
37. Kumar TR, Palapattu G, Wang P, Woodruff TK, Boime I, Byrne MC, Matzuk MM 1999 Transgenic models to study gonadotropin function: the role of follicle-stimulating hormone in gonadal growth and tumorigenesis. Mol Endocrinol 13:851–865
38. Burns KH, Agno JE, Chen L, Haupt B, Ogbonna SC, Korach KS, Matzuk MM 2003 Sexually dimorphic roles of steroid hormone receptor signaling in gonadal tumorigenesis. Mol Endocrinol 17:2039–2052
39. Shikone T, Matzuk MM, Perlas E, Finegold MJ, Lewis KA, Vale W, Bradley A, Hsueh AJ 1994 Characterization of gonadal sex cord-stromal tumor cell lines from inhibin-α and p53-deficient mice: the role of activin as an autocrine growth factor. Mol Endocrinol 8:983–995

40. Xu J, Oakley J, McGee EA 2002 Stage-specific expression of Smad2 and Smad3 during folliculogenesis. Biol Reprod 66:1571–1578
41. Gueripel X, Benahmed M, Gougeon A 2004 Sequential gonadotropin treatment of immature mice leads to amplification of transforming growth factor β action, via upregulation of receptor-type 1, Smad 2 and 4, and downregulation of Smad 6. Biol Reprod 70:640–648
42. Tomic D, Miller KP, Kenny HA, Woodruff TK, Hoyer P, Flaws JA 2004 Ovarian follicle development requires Smad3. Mol Endocrinol 18:2224–2240
43. Xu J, Beyer AR, Walker WH, McGee EA 2003 Developmental and stage-specific expression of Smad2 and Smad3 in rat testis. J Androl 24:192–200
44. Wang RA, Zhao GQ 1999 Transforming growth factor β signal transducer Smad2 is expressed in mouse meiotic germ cells, Sertoli cells, and Leydig cells during spermatogenesis. Biol Reprod 61:999–1004
45. Trudeau VL, Matzuk MM, Hache RJ, Renaud LP 1994 Overexpression of activin-β A subunit mRNA is associated with decreased activin type II receptor mRNA levels in the testes of α-inhibin deficient mice. Biochem Biophys Res Commun 203:105–112
46. Smith JC, Price BM, Van Nimmen K, Huylebroeck D 1990 Identification of a potent *Xenopus* mesoderm-inducing factor as a homologue of activin A. Nature 345:729–731
47. Wittbrodt J, Rosa FM 1994 Disruption of mesoderm and axis formation in fish by ectopic expression of activin variants: the role of maternal activin. Genes Dev 8:1448–1462
48. Meachem SJ, Ruwanpura SM, Ziolkowski J, Ague JM, Skinner MK, Loveland KL 2005 Developmentally distinct in vivo effects of FSH on proliferation and apoptosis during testis maturation. J Endocrinol 186:429–446
49. Nakamura T, Takio K, Eto Y, Shibai H, Titani K, Sugino H 1990 Activin-binding protein from rat ovary is follistatin. Science 247:836–838
50. Cipriano SC, Chen L, Kumar TR, Matzuk MM 2000 Follistatin is a modulator of gonadal tumor progression and the activin-induced wasting syndrome in inhibin-deficient mice. Endocrinology 141:2319–2327
51. Matzuk MM, Bradley A 1992 Cloning of the human activin receptor cDNA reveals high evolutionary conservation. Biochim Biophys Acta 1130:105–108
52. Wu TC, Jih MH, Wang L, Wan YJ 1994 Expression of activin receptor II and IIB mRNA isoforms in mouse reproductive organs and oocytes. Mol Reprod Dev 38:9–15
53. Kumar TR, Wang Y, Matzuk MM 1996 Gonadotropins are essential modifier factors for gonadal tumor development in inhibin-deficient mice. Endocrinology 137: 4210–4216
54. Matzuk MM, Finegold MJ, Mishina Y, Bradley A, Behringer RR 1995 Synergistic effects of inhibins and Mullerian-inhibiting substance on testicular tumorigenesis. Mol Endocrinol 9:1337–1345
55. Mishina Y, Rey R, Finegold MJ, Matzuk MM, Josso N, Cate RL, Behringer RR 1996 Genetic analysis of the Mullerian-inhibiting substance signal transduction pathway in mammalian sexual differentiation. Genes Dev 10: 2577–2587
56. Shou W, Woodruff TK, Matzuk MM 1997 Role of androgens in testicular tumor development in inhibin-deficient mice. Endocrinology 138:5000–5005
57. Burns KH, Agno JE, Sicinski P, Matzuk MM 2003 Cyclin D2 and p27 are tissue-specific regulators of tumorigenesis in inhibin α knockout mice. Mol Endocrinol 17: 2053–2069
58. Cipriano SC, Chen L, Burns KH, Koff A, Matzuk MM 2001 Inhibin and p27 interact to regulate gonadal tumorigenesis. Mol Endocrinol 15:985–996
59. Finkelstein JS, O'Dea LS, Whitcomb RW, Crowley Jr WF 1991 Sex steroid control of gonadotropin secretion in the human male. II. Effects of estradiol administration in normal and gonadotropin-releasing hormone-deficient men. J Clin Endocrinol Metab 73:621–628
60. Clotman F, Lemaigre FP 2006 Control of hepatic differentiation by activin/TGFβ signaling. Cell Cycle 5:168–171
61. Yasuda H, Mine T, Shibata H, Eto Y, Hasegawa Y, Takeuchi T, Asano S, Kojima I 1993 Activin A: an autocrine inhibitor of initiation of DNA synthesis in rat hepatocytes. J Clin Invest 92:1491–1496
62. Schwall RH, Robbins K, Jardieu P, Chang L, Lai C, Terrell TG 1993 Activin induces cell death in hepatocytes in vivo and in vitro. Hepatology 18:347–356
63. Knight PG, Muttukrishna S, Groome NP 1996 Development and application of a two-site enzyme immunoassay for the determination of 'total' activin-A concentrations in serum and follicular fluid. J Endocrinol 148:267–279
64. O'Connor AE, McFarlane JR, Hayward S, Yohkaichiya T, Groome NP, de Kretser DM 1999 Serum activin A and follistatin concentrations during human pregnancy: a cross-sectional and longitudinal study. Hum Reprod 14: 827–832
65. Pangas SA, Li X, Robertson EJ, Matzuk MM 2006 Premature luteinization and cumulus cell defects in ovarian-specific Smad4 knockout mice. Mol Endocrinol 20: 1406–1422
66. Livak KJ, Schmittgen TD 2001 Analysis of relative gene expression data using real-time quantitative PCR and the $2(-\Delta\ \Delta\ C(T))$ method. Methods 25:402–408
67. Li Q, Kumar R, Underwood K, O'Connor AE, Loveland KL, Seehra JS, Matzuk MM, Prevention of cachexia-like syndrome development and reduction of tumor progression in inhibin-deficient mice following administration of a chimeric activin receptor type II-murine Fc protein. Mol Hum Reprod, in press

Molecular Endocrinology **is published monthly by The Endocrine Society (http://www.endo-society.org), the foremost professional society serving the endocrine community.**